JOURNAL OF MATERIALS SCIENCE: MATERIALS IN MEDICINE 1 (1990) 69–80

The response of the hierarchical structure of the intervertebral disc to uniaxial compression

J. J. CASSIDY*, A. HILTNER, E. BAER
Department of Macromolecular Science and Center for Applied Polymer Research, Case Western Reserve University, Cleveland, Ohio 44106, USA

The time-dependent mechanical response of the canine intervertebral disc in axial compression is related to the response of the various levels of the hierarchical organization. In stress relaxation the initial transverse bulging of the disc recovers almost completely with time. The corresponding decrease in volume correlates with the measured loss of water from the disc. The three-dimensional architecture of the disc, examined by sectioning isolated discs that had been fixed in compression, accommodates the volume displacement. Bulging of the peripheral lamellae is minimized by the curvature of the vertebral interface and by stress-driven transport of water out of the disc through the cartilage end-plates into the vertebral bodies. Even though the disc undergoes macroscopic compression, the fibres of the lamellae are loaded in tension and their mode of deformation is compared with that of other connective tissues such as tendon and intestine.

1. Introduction

It was recently shown that the annulus fibrosus, the outer component of the intervertebral disc that is made up of discrete layers or lamellae of fibrous collagen, has a hierarchical structure with gradient characteristics at the various levels of organization [1]. It is known well that the fibres of the lamellae are tilted with respect to the spinal axis; it is not known so well that the fibres possess a planar crimped waveform similar to that of tendon [2] and intestine [3]. Relationships between the hierarchical structure and mechanical function in these connective tissues have been developed by analysing the response at the various levels of organization under the appropriate stress state.

Axial compression, in addition to torsion and bending, is a mode of deformation normally experienced by the disc. Many aspects of the mechanical behaviour of isolated lumbar segment in compression have been reported [4, 5], including the time-dependent viscoelastic response [6, 7]. Differences in the mechanical response between thoracic and lumbar discs have been reported [8], but the scatter among individual discs sometimes overshadowed the differences along the spine [9].

Attempts have been made to relate the mechanical response of the disc to some aspects of the structure. At the macroscopic level, radial bulging of the disc around its circumference has been measured under various loading conditions, primarily to characterize biomechanical aspects of pathological conditions and therapautic measures [10, 11].

It is generally believed that compressive forces are transmitted across the disc to the fibres of the outer lamellae, which are held in tension. Although the nucleus is thought to play a major role in the transmission of forces, the restoring force of the stretched fibres is considered to balance the effects of nuclear pressure [12, 13]. The contribution of water to the compressive properties of the disc has also been discussed. Water is expressed from the disc when it is compressed, and is re-imbibed when the load is removed [14]. Creep and stress relaxation are often attributed to the squeezing out of fluid, but the relative influence of the annulus to the viscoelastic properties is seldom considered in conjunction with fluid loss [15].

The purpose of this investigation was to examine the role of the various levels of structural organization in the response of the isolated disc to compressive loading. Stress–strain measurements over a range of loading rates, in addition to stress-relaxation experiments to characterize the viscoelastic behaviour, were performed. Fluid loss was also determined and related to the response of the annulus and the mechanical behaviour of the disc.

2. Experimental methods

Spinal segments were harvested from adult mongrel canines. Discs from six spines were used to determine the effect of spinal location on the mechanical properties. Unless noted, all further tests were done on discs in the thoracolumbar and lumbar regions and, when appropriate, adjacent discs were used in order to minimize variation due to spinal location. Two spines were used to determine the rate-dependence of the mechanical properties. Four spines were used in the stress-relaxation tests and measurements were carried out at

* *Present address:* Richards Medical Co., Memphis, Tennessee 38116, USA.

0957–4530/90 $03.00 + .12

two loads on adjacent discs from two locations: thoracic and lumbar. The water content and disc geometry were examined in additional spines not used in the mechanical test procedures.

Isolated disc specimens were prepared by cutting transversely through the vertebral bones above and below the disc. The posterior articulating facets and pedicles were removed. The resultant test specimens consisted of a disc with approximately 10 mm viable bone above and below. Discs were enclosed in plastic until tests, in order to maintain 100% relative humidity, and specimens were used fresh or kept refrigerated at 4° C. All were tested within 72 h of removal. Before testing, specimens were equilibrated at room temperature. The discs were kept sealed in plastic throughout the tests.

The disc height was measured at the periphery. The area of the disc was determined by measuring the maximum width of the disc and the length along the sagittal plane, then applying the area formula for an ellipse. An empirically determined correction factor was used to account for deviation of the disc from this idealized geometry and added 10% to the cross-sectional area calculated. The disc volume was calculated as the volume of an elliptical cylinder with height at the periphery. A correction factor for that portion of the cylindrical volume occupied by vertebral bone was determined empirically. This equalled a 12.5% reduction in the initial volume.

Low-strain-rate mechanical tests were conducted using a screw-driven Instron 1123 mechanical testing machine. For high-strain-rate tests a servo-hydraulic Instron 1331 mechanical testing machine was used. Specimens were placed between solid loading platens and preloaded to a stress of 0.1 MN m^{-2}. Disc specimens used to study the effect of location were compressed at a rate of 5 mm min^{-1}, a maximum stress was achieved and a decrease in stress was observed. Specimens for stress-relaxation were compressed at a rate of 200 mm sec^{-1} to the desired strain and maintained at that strain for 30 min while the stress was monitored continuously.

The water content in the disc was measured by dissecting the disc away from the bone before it was freeze-dried. A weight percentage was calculated as the difference in weight before and after freeze-drying divided by the initial weight. The water loss from the disc under strain was measured by compressing a test specimen and holding it in a clamp at 100% humidity and room temperature. After 2 h the disc was dissected out and freeze-dried to measure the water content. A total of approximately 60 discs from six spines were dissected into anterior, lateral and posterior regions of the annulus fibrosus and the nucleus pulposus in order to determine the regional water content of the disc.

Preserved disc specimens were sectioned for histological examination. Some specimens were clamped in compression before immersion in formalin (40% formaldehyde solution) for 48 h. It was anticipated that fixation occurred sufficiently slowly that these specimens were fixed in the stress-relaxed state. Slices were taken along the transverse and sagittal anatomic directions and in the circumferential direction by cutting a chord through the annulus fibrosus. Additional slices were cut through the annulus parallel to the collagen fibres to measure the parameters of the crimp waveform. Transmission optical microscopy was used to examine the disc specimens over a range of magnifications from 10× to 1000×. The crimp angle, period and length were measured using crossed polarized light as in the previously reported methodology [1].

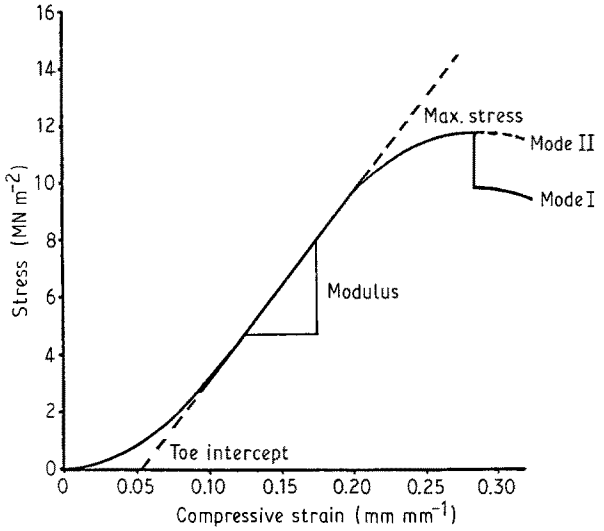

Figure 1 Stress–strain curve of intervertebral disc in compression, showing toe, linear and yield regions.

3. Results and discussion

3.1. Stress–strain behaviour

The stress–strain curve in compression of a representative intervertebral disc specimen is shown in Fig. 1. The S-shaped curve may be divided into three regions. The initial response is characterized by a gradually increasing modulus with increasing strain; this toe region extends to approximately 0.10 strain. It is followed by a linear region of constant modulus that extends from the end of the toe region to about 0.20 strain. Finally, at high strains, the modulus begins to decrease gradually with increasing strain; this yield region continues until the disc fails.

Two modes of failure are observed in the intervertebral disc specimens. In the yield region of the stress–strain curve the specimen may attain a maximum stress value then drop sharply to a lower stress (mode I failure) or it may simply decline gradually with increasing strain (mode II failure). In mode I failure an audible popping or cracking sound often accompanies the drop in stress. This condition is seen in about 66% of the discs tested. No sound is heard from those specimens exhibiting the gradual decrease in stress. When specimens are dissected and examined grossly in the optical microscope, discs exhibiting a sharp stress-drop usually have ruptured the cartilage end-plates and material from the nucleus pulposus has been forced into the vertebral bodies. In those discs where a gradual decrease in stress is noted, fissures appear in the fibrous lamellae of the annulus fibrosus, allowing nuclear material to move laterally through the disc. In some cases gel from the nucleus has penetrated the full thickness of the annulus and appears on the outer surface of the disc. This usually

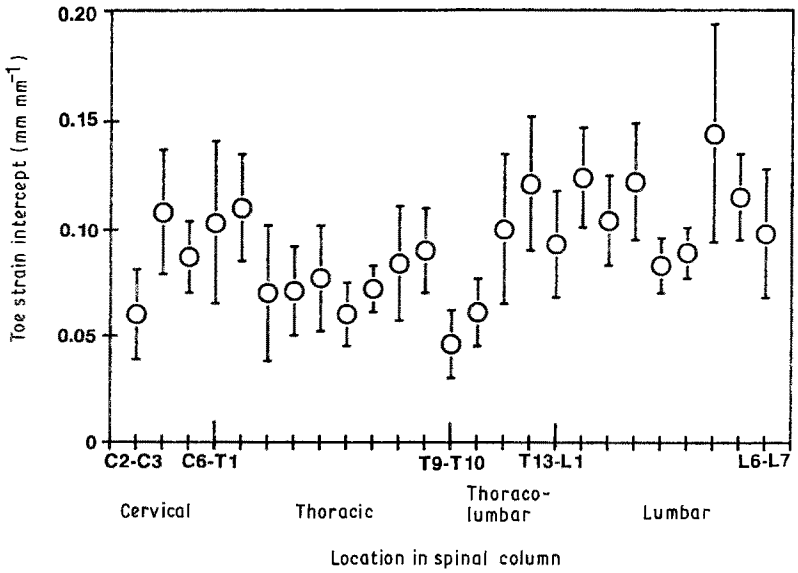

Figure 2 Compressive toe intercept strain plotted against location in the spinal column. The loading rate was 5 mm min^{-1}. The bars indicate the standard deviation.

occurs at the posterior aspect of the disc where the lamellae are thinnest.

The stress–strain response of the disc to compression was examined at each level in the spinal column from C2–C3 to L6–L7 in six spines. the upper limit of the toe region of the stress–strain curve does not change with location in the spinal column, having a mean value of 0.15 ± 0.02. The toe strain intercept, as determined by extrapolating the linear portion of the stress–strain curve to the strain axis, similarly does not vary with location, having a mean value of 0.09 ± 0.02 (Fig. 2).

The modulus in the linear region increases by a factor of 3 over the length of the spinal column from 32 MN m^{-2} at C2–C3 to 115 MN m^{-2} at L6–L7 (Fig. 3). Variability in the data reflects the differences among spines from different canines. Although a linear regression fits the data with $r = 0.95$, the plot suggests that a more complex relationship exists between location and modulus. In particular, there appears to be a sharp increase in modulus from the thoracolumbar to the lumbar region.

The maximum stress in compression more than doubled over the length of the spinal column from 8 MN m^{-2} at C2–C3 to 19 MN m^{-2} at L5–L6, whereas the maximum stress of the L6–L7 disc was markedly lower than that of the other lumbar discs (Fig. 4). Again, a linear regression describes the data with an r-value of 0.95, but like the modulus, the maximum stress appears to increase sharply from the thoracolumbar to the lumbar region.

3.2. Rate dependence of mechanical properties

The experiments on the variation in properties with location in the spinal column were carried out at a moderate loading rate of 5 mm min^{-1}. Additional specimens were tested to failure at slower loading rates of 0.005, 0.05 and 0.5 mm min^{-1} and at higher loading rates of 50 and 500 mm min^{-1}. These produced a range of strain rates from approximately 0.001 to 100 min^{-1} Specimens for these experiments were taken from the thoracolumbar and lumbar regions, where the dependence of the mechanical properties on location was minimal. The data points on the following plots usually represent results from compression of two discs; the standard deviation is within the area of the marker. The toe strain of the disc did not change with the loading rate in these tests, having a mean value of 0.12 ± 0.01. The toe intercept strain similarly did not change with loading rate (Fig. 5), with a mean value of 0.07 ± 0.01. These values are somewhat

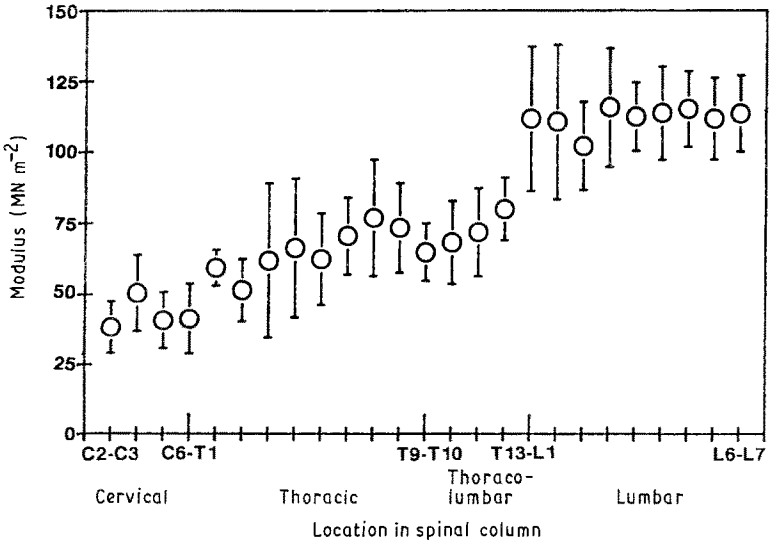

Figure 3 Compressive modulus plotted against location in the spinal column. The loading rate was 5 mm min^{-1}. The bars indicate the standard deviation.

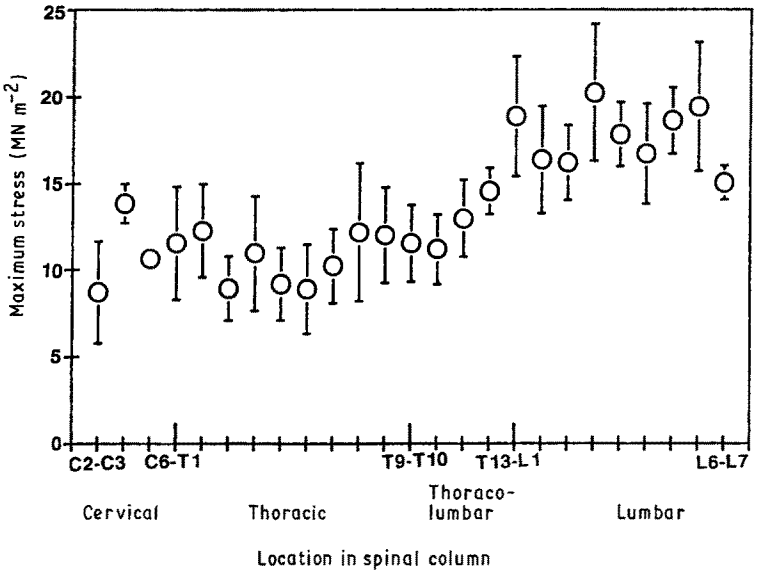

Figure 4 Compressive maximum stress plotted against location in the spinal column. The loading rate was 5 mm min^{-1}. The bars indicate the standard deviation.

lower than the strains reported for the previous experiments on the variation of mechanical properties with location in the spinal column. Apparently, these tests were conducted on discs from two animals whose toe strains represent the lower limit of the normal range in the canine.

The compressive modulus, E, of the disc increases with increasing loading rate from about 40 MN m^{-2} at 0.005 mm min^{-1} to 135 MN m^{-2} at 500 mm min^{-1} (Fig. 6). This more than three-fold increase in modulus is linear with loading rate, regression analysis (r = 0.99) of the data indicates a functional relationship of

$$E = 17 \times \log(\text{rate}) + 93$$

The maximum compressive stress, σ_{max}, achieved during testing also increased with increasing loading rate from about 5 MN m^{-2} at a rate of 0.005 mm min^{-1} to 19 MN m^{-2} at 500 mm min^{-1} (Fig. 7). This change is also linear with loading rate, regression analysis (r = 0.99) of the data yields the relationship

$$\sigma_{max} = 2.6 \times \log(\text{rate}) + 13$$

The strong rate-dependence of the linear and failure regions is not observed in the toe region. That the latter is characterized by low stresses over a significant range of strain supports the conclusion that the time-dependence is stress- rather than strain-dependent.

3.3. Stress relaxation

The stress-relaxation response of the disc deformed to a constant macroscopic strain was examined using specimens prepared according to the same protocol described for discs tested to failure. Macroscopic strains of 0.05 and 0.15 were selected because they represent the centre of the toe and linear regions of the stress–strain curve, respectively. In addition, two locations in the spine, thoracic and lumbar, were examined. Discs deformed to both 0.05 and 0.15 strain relax to < 10% of the initial stress in approximately 30 min. At both 0.05 and 0.15 strain there is no significant difference in the response of thoracic and lumbar discs. If the experimental data are normalized to the initial stress, all of the stress-relaxation curves can be superimposed to create a master curve describing the relaxation response. The master curve in Fig. 8 is drawn through the mean normalized stress at various points on the relaxation curve. The shape of the stress–time curve does not fit a simple exponential relationship; the shape of the relaxation curve is discussed in a companion paper [16].

During the stress-relaxation experiments, outwards deformation of the disc was measured at the anterior,

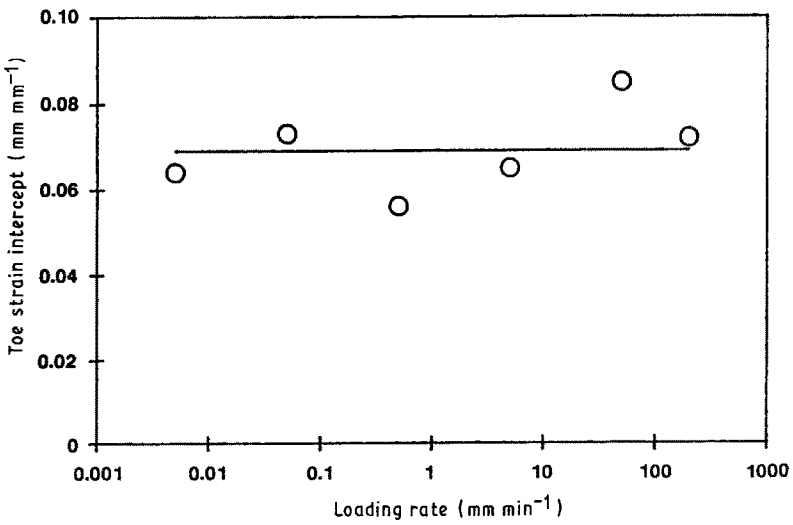

Figure 5 Compressive toe intercept strain plotted against loading rate.

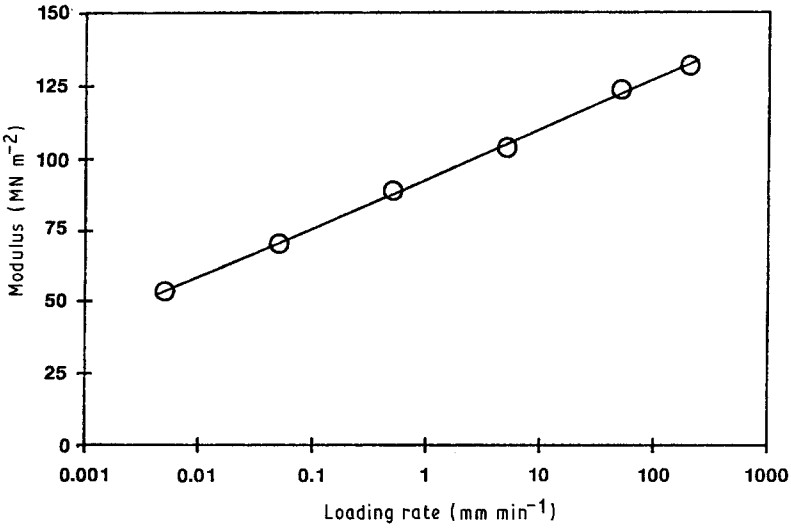

Figure 6 Compressive modulus plotted against loading rate.

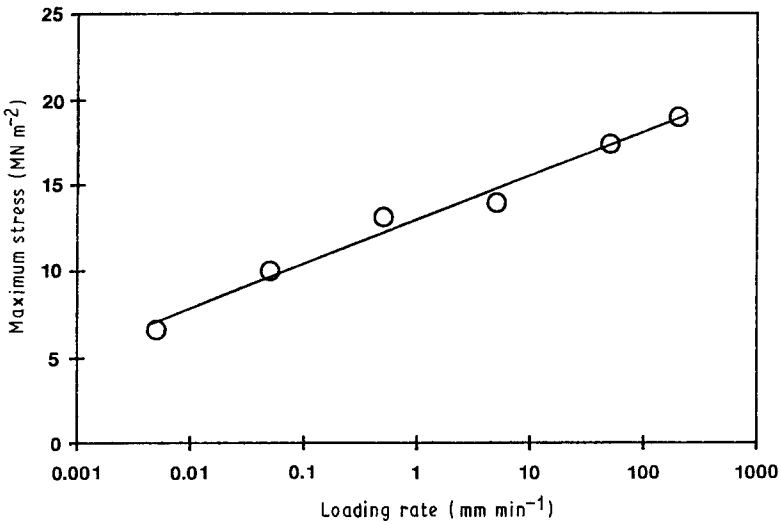

Figure 7 Compressive maximum stress plotted against loading rate.

lateral and posterior aspects of the disc by using dial gauges. Outwards bulging was recorded as a function of time during the test and normalized to the initial dimensions of the specimen. A large variability among individual discs was encountered. However, some qualitative conclusions may be drawn. Bulging is not symmetrical around the periphery of the disc. In general, at 0.05 strain the anterior and lateral aspects of the disc bulge approximately equally, whereas the posterior bulges slightly less. This bulge is 0.10 to 0.25 mm at the anterior and lateral and 0.05 to 0.20 mm at the posterior for discs that consistently measure about 17 mm × 12 mm. At 0.15 strain the anterior bulges slightly more than the lateral. Both bulge to a much greater extent than the posterior annulus, where there is no increase over the 0.05 strain. The anterior bulges 0.50 to 1.00 mm, the lateral 0.30 to 0.70 mm and the posterior 0.05 to 0.20 mm.

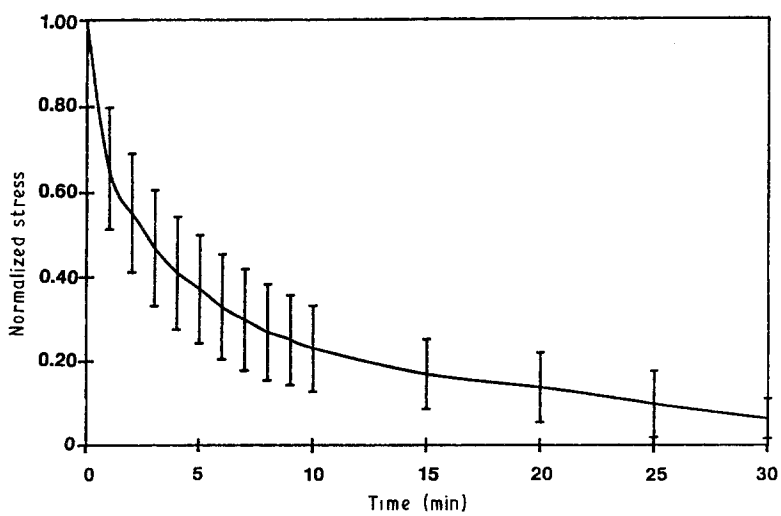

Figure 8 Master relaxation curve of normalized stress against time.

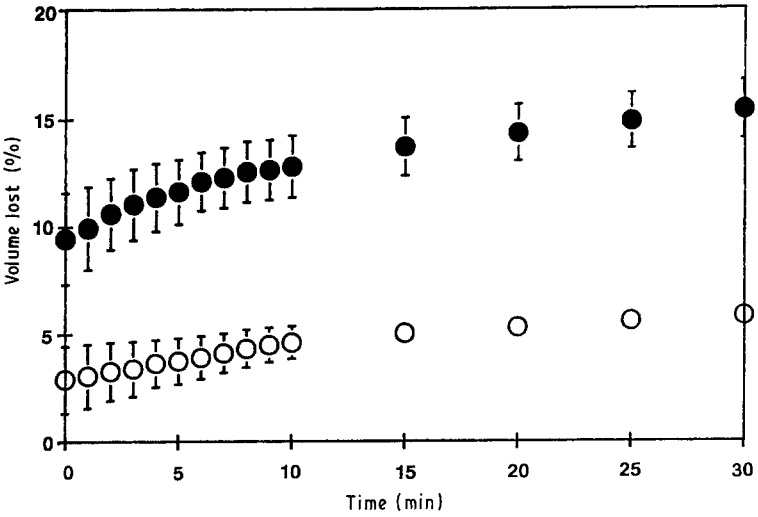

Figure 9 Decrease in disc volume with time as calculated from bulge measurements during stress relaxation. (●) 15% and (○) 5% compression.

The bulge decreases with time as the stress relaxes. At 0.05 compression the bulge is recovered almost entirely after 30 min and the cross-sectional area returns to its initial dimensions. At 0.15 compression some residual bulge remains after 30 min. This is 0.01 mm or less for the anterior and lateral. The posterior recovers only slightly, if at all.

The decrease in the volume of the disc with time is calculated using these dimensional changes (Fig. 9). The volume lost by the disc at 30 min at 0.05 strain is about 5.1%. At 0.15 strain the volume lost is 15.0% Within experimental error, the volume change compensates almost entirely for the imposed strain.

3.4. Water content

The highest water content is in the nucleus pulposus which is 82 ± 3% water by weight. In contrast, the annulus fibrosus averages 62 ± 4% water at the anterior position and the lateral and posterior regions of the annulus both average 68 ± 2% water. Further subdivision of these regions shows a variation in water content through the annulus. It is always lowest at the periphery (Table I) and increases from the periphery to the centre of the annulus. In the posterior and lateral positions further changes in the water content between the centre of the annulus and the nucleus are small. The anterior position differs in this regard and the water content decreases near the nucleus. The region of highest water content coincides with an acute narrowing in the anterior of the disc near the centre of the annulus.

The water content in all regions of the disc is lower after the disc has been held in compression for a time. The water content decreases gradually as the strain increases so that when compressed to 0.20 strain the overall water content of the annulus is close to 50% and that of the nucleus about 70% (Fig. 10). Further subdivision of the annulus showed that the least water is lost at the periphery (Table I) and water is preferentially lost from regions in the centre of the annulus or near the nucleas that initially have the highest water content. This has the effect of creating a more uniform distribution of water through the annulus, so that at 0.20 compressive strain the water content in most regions is in the range 50 to 60%.

The water content is used to estimate the weight change during compression, and is reported in Table II as the fractional change in the initial weight of the disc. If the weight fractions are taken to be approximately equal to the volume fractions, the comparison in Table II with the volume change measured directly from the bulging shows that water loss compensates for essentially the entire volume change. Although the environment is maintained at 100% relative humidity in order to minimize evaporation, no condensed water could be detected on the peripheral surfaces of the discs during compression. When the compressed specimens were removed from the test fixture, however, it was observed that a mixture of fluids had been exuded from the cut ends of the vertebral bodies and deposited on the loading platens. These two observations suggest that the principal pathway by which water is lost from the disc is through the cartilage end-plates into the vertebral bodies, rather than transversely through the disc surface.

It is proposed that the mechanism responsible for the viscoelastic character of the disc response in compression, as manifested in the stress-relaxation

TABLE I Water content (wt %) of the disc at various locations

Location	Periphery	Centre	Inner	Overall
0.00 Compressive strain				
Anterior annulus	57 ± 3	74 ± 3	64 ± 4	62 ± 4
Lateral annulus	60 ± 3	77 ± 2	74 ± 3	68 ± 2
Posterior annulus	59 ± 3	67 ± 4	71 ± 3	68 ± 2
Nucleus pulposus				82 ± 3
0.20 Compressive strain				
Anterior annulus	53 ± 3	60 ± 5	54 ± 4	50 ± 4
Lateral annulus	54 ± 4	57 ± 6	59 ± 5	54 ± 5
Posterior annulus	52 ± 4	50 ± 5	48 ± 4	53 ± 4
Nucleus pulposus				71 ± 4

TABLE II Total water loss against compressive strain

Strain	Weight loss as water* ($g\,g^{-1}$)	Volume change from bulging† ($cm^3\,cm^{-3}$)
0.05	0.045 ± 0.002	0.051 ± 0.003
0.10	0.088 ± 0.003	
0.15	0.130 ± 0.005	0.150 ± 0.013
0.20	0.177 ± 0.007	

*Relaxed 2 h; †relaxed 30 min.

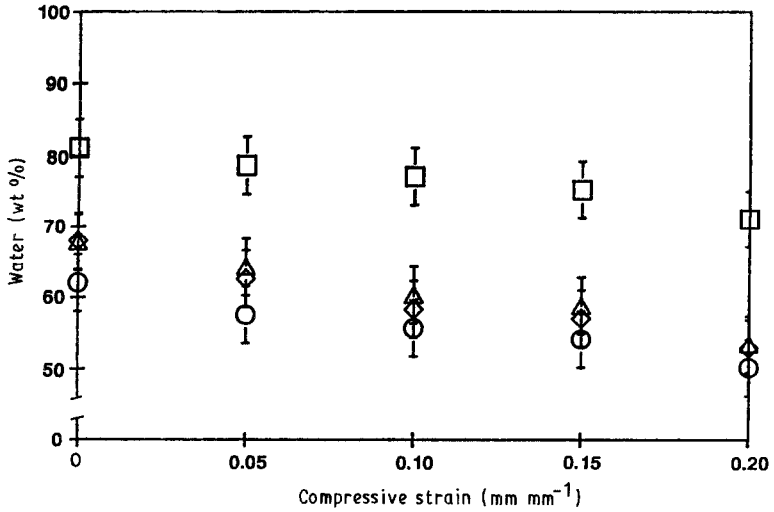

Figure 10 Water content of the disc plotted against compressive strain. (□) Nucleus, (◇) posterior, (△) lateral and (○) anterior.

behaviour and the rate-dependence of modulus and strength, is the transport of water out of the disc through the cartilage end-plates into the vertebral bone. This hypothesis is supported by experimental data on the dimensional changes in the disc during stress relaxation and confirmed by direct measurement of the water content of compressed discs. Under physiological conditions, instead of being exuded through the cut ends of the vertebral bodies, the water transported through the end-plates is seen as being absorbed into the vascular system, from which it could be restored to the disc when the stress is removed. This hypothesis accommodates the requirement for reversibility, although the recovery could not be confirmed experimentally with the excised disc system.

3.5. Response of the hierarchical structure to compression

The structural elements of the disc hierarchy could not be observed directly during compressive deformation. Instead, discs that had been fixed as they were held in compression were sectioned and examined histologically. The shape of the disc in cross-section varies with the location in the spinal column. In the cervical region the discs are elliptical and the nucleus pulposus is slightly off-centre, being closer to the posterior than the anterior. In the thoracic, thoracolumbar and lumbar regions the discs are kidney-bean shaped (Fig. 11a). The nucleus is also kidney-bean shaped and is found posterior to the centre of the disc, so the annulus fibrosus is thicker at the anterior and lateral aspects and thinner at the posterior. This corresponds to the relative thickness of the lamallae, since the number of lamellae is the same at all positions around the circumference of the disc [1].

In sagittal sections the interface between the vertebral bodies and the disc has a complex shape. Considering first the anterior aspect, the interface is curved so that the disc height gradually decreases from the periphery to a point halfway between the periphery of the disc and the centre of the nucleus, where the disc height is approximately half the height at the periphery. The disc height gradually increases again further inwards towards the centre of the nucleus, but does not regain the original height at the periphery (Fig. 11b). The region of the cartilage end-plate to which lamellae of the annulus are anchored distinctly extends inwards past the narrowest part of the disc. Lamellae in the anterior aspect are straight up-and-down or bulged slightly outwards. By comparing the photomicrograph of the unloaded disc in Fig. 12a with those in Figs 12b to d of discs loaded to 0.20 strain, it can be seen that the lamellae peripheral to the narrowest part of the disc have a distinct outwards bulge in the compressed state. Closer to the nucleus the orientation of the compressed lamellae varies from one disc to another; the lamellae can be bulged outward (Fig. 12b), bulged inwards (Fig. 12c) or buckled (Fig. 12d). Deformation of the lamellae in this inner region of the anterior aspect is emphasized by the relatively high compressive strain that must be accommodated by the narrowest part of the disc. The variety

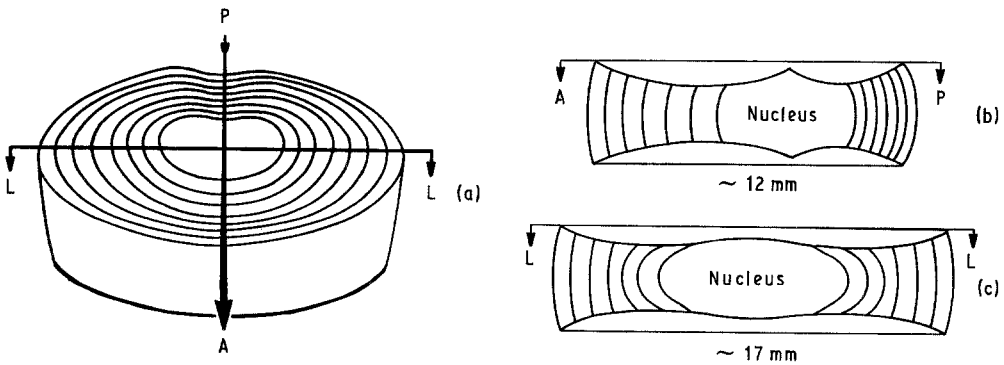

Figure 11 Schematic diagram showing the shape of the disc and the vertebral interface. (a) Disc isolated from vertebral bodies, (b) anterior–posterior section and (c) lateral section.

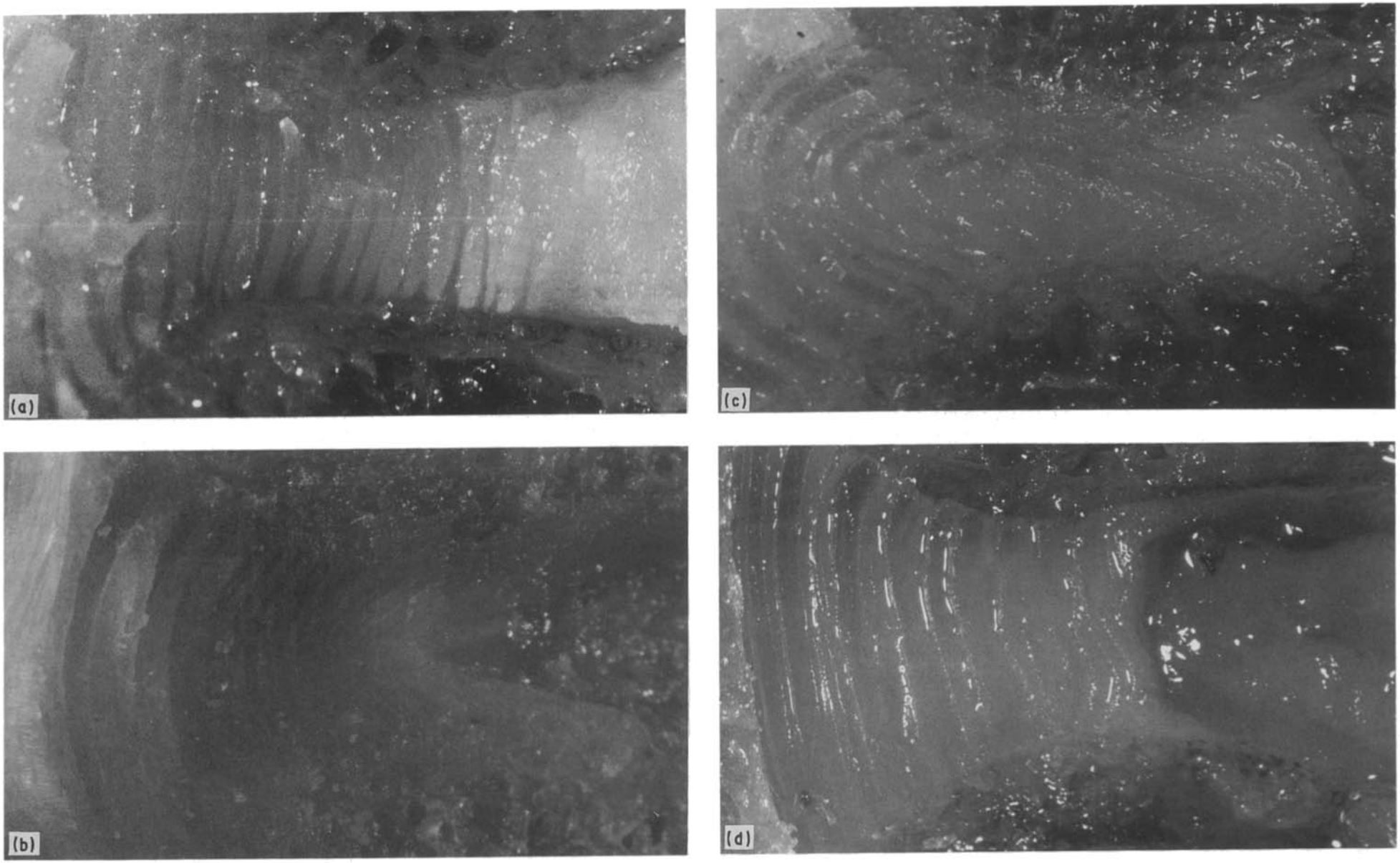

Figure 12 Photomicrographs obtained with the stereo optical microscope of the anterior annulus showing lamellar bulging and buckling. Magnification 35 ×. (a) With no load and (b to d) loaded to 0.20 compressive strain.

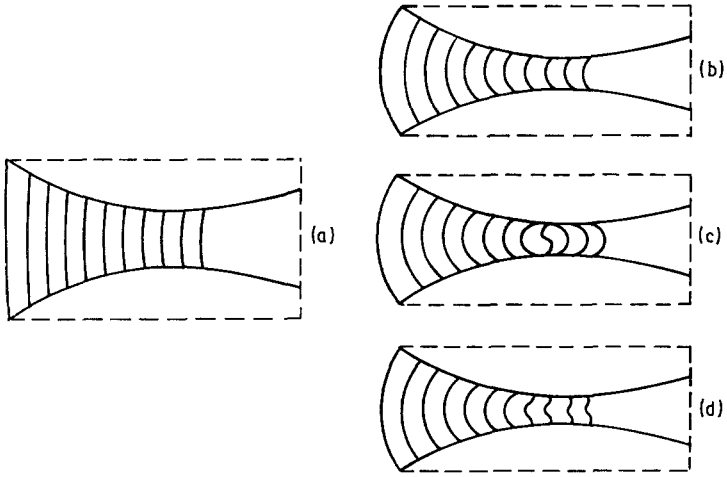

Figure 13 Schematic representation of lamellar bulging and buckling at the anterior aspect of the annulus. (a) With no load and (b to d) loaded to 0.20 compressive strain.

of orientations assumed by the compressed lamellae, shown schematically in Fig. 13 is attributable to several factors. For example, the curvature of the vertebral interface in this region encourages the lamellae to bulge inwards as they are compressed, but spreading of the nucleus pushes them outwards and the straight up-and-down orientation in the unloaded disc does not predispose the lamellae to bend preferentially in either direction. As a result, several possible modes of deformation are observed.

The vertebral interface at the posterior aspect is also curved, and in this case the curvature is more severe than at the anterior aspect because the annulus is thinner (Fig. 11b). Lamellae of the annulus extend only from the periphery to the narrowest part of the disc and are bulged slightly outwards. When photomicrographs of the posterior region are compared, one from a disc with no load applied and the other from an adjacent disc that was fixed at a strain of 0.20 (Fig. 14), the outwards bulge is seen to become more severe as the disc is compressed. The change in lamellar orientation at the posterior aspect following compression is shown schematically in Fig. 15.

The disc is much flatter at the lateral aspect than at either the anterior or posterior aspects, although there is enough curvature of the vertebral interface to make the disc distinctly thicker at the periphery (Fig. 11c). Lamellae at the periphery are straight, whereas those close to the nucleus bulge outwards; when compressed, outer lamellae buckle whereas inner lamellae bulge sharply outwards (Fig. 16). Typical orientations of the lamellae at the lateral aspect are shown in Fig. 17.

Fibres of the lamellae are oriented at an angle to the spinal axis and have a planar crimped waveform [1]. The crimped waveform, seen in transverse sections cut parallel to the interlamellar angle (Fig. 18), progressively straightens as the disc is compressed, although completely uncrimped fibres are not observed even at a strain of 0.20. The parameters that characterize the crimp were measured at various positions of the annulus at increasing strains. The data for the eighth lamella from the periphery at the anterior–lateral aspect are typical (Fig. 19); they show the gradual decrease in crimp angle and increase in crimp period as the fibres uncrimp with increasing strain. In addition, the slight increase in interlamellar angle at this position in the annulus, from about 63° at rest to 70° when the strain is 0.20, reveals some reorientation of the fibres away from the spinal axis.

Previous studies have described a hierarchical structure for the annulus fibrosus of the human disc, with gradients through the thickness at the various levels of organization [1]. Lumbar discs of the canine are about

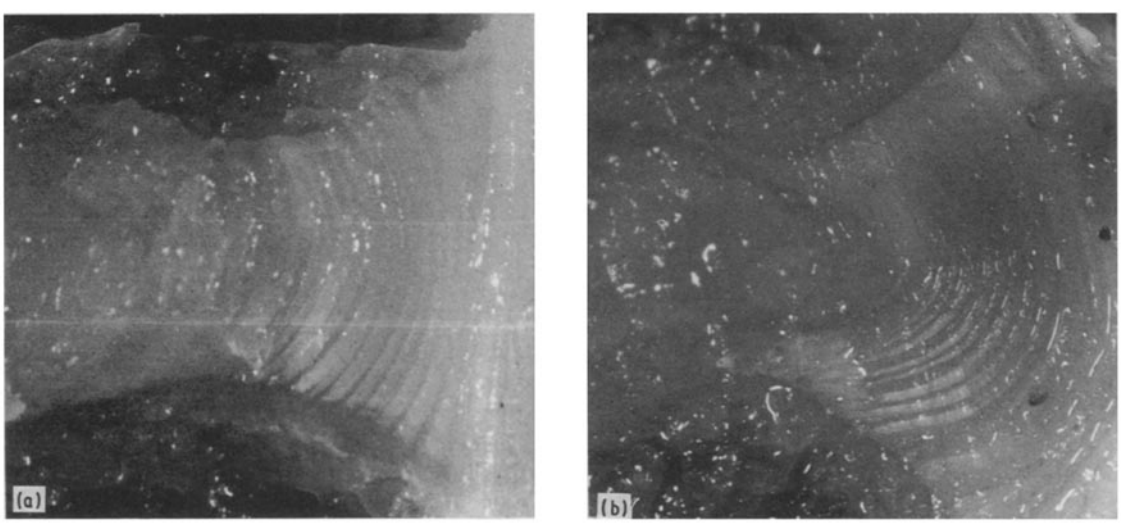

Figure 14 Photomicrographs obtained with the stereo optical microscope of the posterior annulus showing lamellar bulging. Magnification 28 ×. (a) With no load and (b) loaded to 0.20 compressive strain.

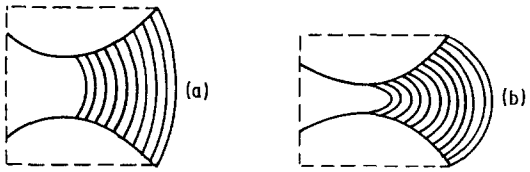

Figure 15 Schematic representation of lamellar bulging at the posterior aspect of the annulus. (a) With no load and (b) loaded to 0.20 compressive strain.

one-third smaller in cross-sectional area but the kidney-bean shape resembles that of the human disc and the 4:1 volume ratio of annulus to nucleus is also the same. The average number of lamellae is about 40 in both human and canine discs; lamellae are distinctly thinner at the posterior in both species and the inter-lamellar fibre orientation is the same. The fibres of the canine lamellae also exhibit the planar crimped waveform that was described recently [1], and the characteristic parameters of crimp angle and period are similar to those of the human. It is anticipated that the deformation modes observed with the readily available canine disc will be relevant to the understanding of the behaviour of the human disc, because of the close resemblance between the hierarchical structures of the human and canine lumbar discs.

It is now possible to suggest how the three-dimensional architecture of the disc responds to compressive loading. Although direct observations of the hierarchical structure are made on relaxed discs that have experienced significant reduction in volume due to water loss, the process by which this relaxed state is

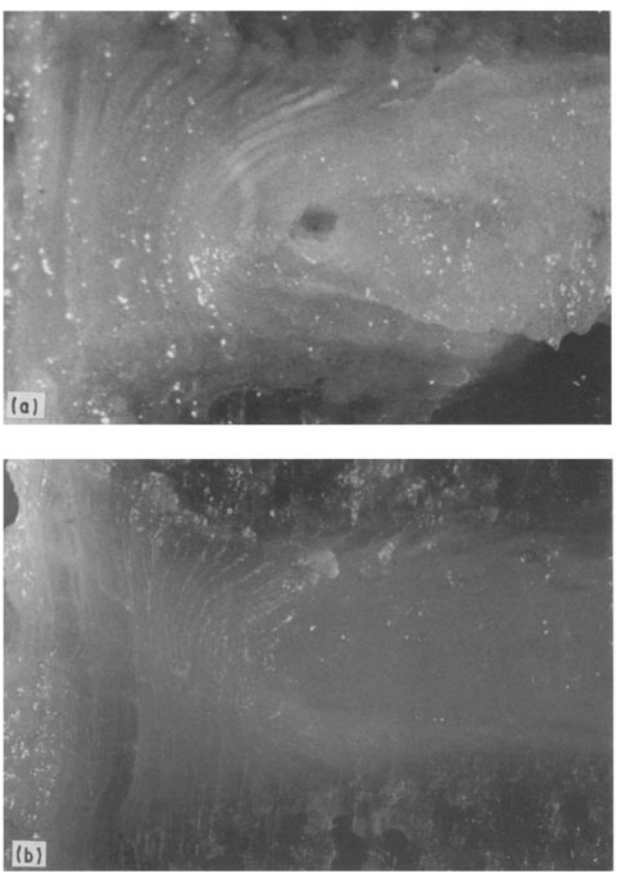

Figure 16 Photomicrographs obtained with the stereo optical microscope of the lateral annulus showing lamellar bulging and buckling. Magnification 28 ×. (a) With no load and (b) loaded to 0.20 compressive strain.

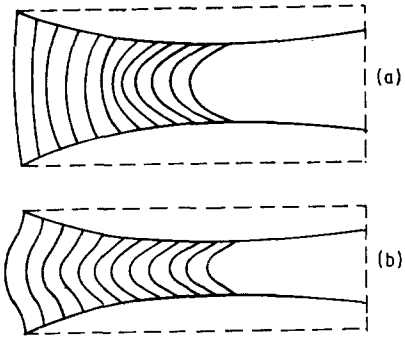

Figure 17 Schematic representation of lamellar bulging and buckling at the lateral aspect of the annulus. (a) With no load and (b) loaded to 0.20 compressive strain.

achieved can be imagined to occur as follows. Initially, before the volume is altered by transport of water out of the disc, lateral spreading of the nucleus forces the lamellae to deflect outwards. The disc is not isotropic in cross-section, and the amount of bulging is distinctly less at the posterior aspect than at either the lateral or anterior aspects. Since the fibres of the lamellae are anchored in the cartilage end-plates, the lamellae accommodate the transverse strain by bulging outwards. Proceeding outwards from the nucleus, a cumulative increase in the amount of bulging is required by the compressive strain, so if the disc were of uniform height, peripheral lamellae would be required to bulge considerably more than inner lamellae. The curved shape of the vertebral interface which causes the disc height to be greatest at the periphery, results in a smaller compressive displacement, as a fraction of the disc height, at the periphery than near the nucleus; since less bulge is therefore required of the peripheral lamellae to respond to the compressive strain, they can

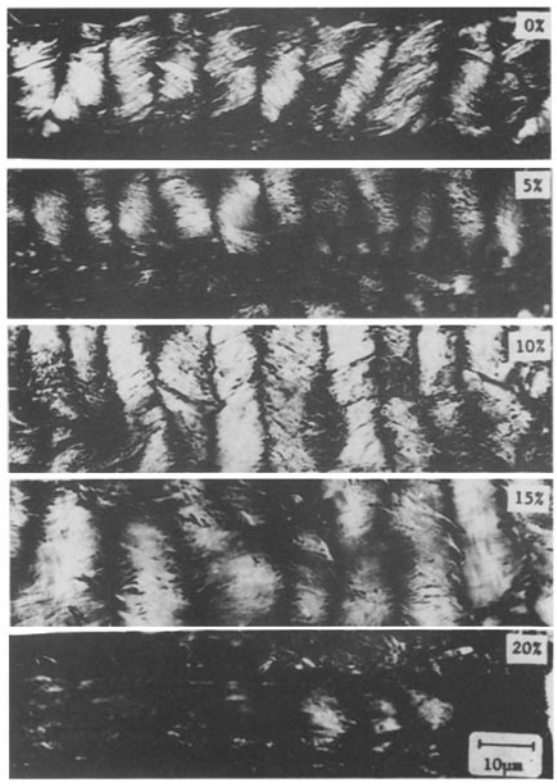

Figure 18 The crimped collagen fibres of the peripheral annulus fibrosus at various compressive strains as viewed in the polarizing optical microscope.

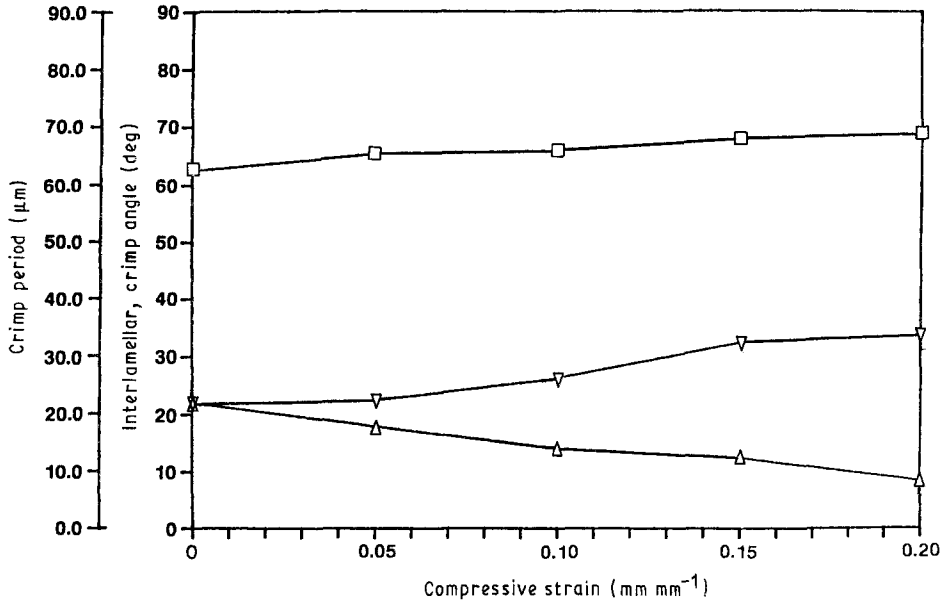

Figure 19 Crimp parameters and interlamellar angle as a function of compressive strain. (□) Interlamellar angle, (▽) crimp period and (△) crimp angle.

more easily accommodate the additional bulging imposed by the inner lamellae.

When water flows out of the disc through the cartilage end-plates into the vertebral bone, the outwards bulge of the annulus is relieved. It is significant that the water content is highest in the nucleus and the inner regions of the annulus, since these regions are observed to lose more water and hence undergo a larger volume decrease than the outer regions of the annulus during stress relaxation. As the volume is reduced, the lamellae are no longer forced to bulge outwards and they buckle to conform to the smaller separation of the vertebral bodies.

The fibres of the lamellae are constrained at the cartilage end-plates, so they must extend in length to accommodate the bulging. Even though the disc undergoes macroscopic compression, the fibres of the lamellae are loaded in tension and their mode of deformation can be compared with other connective tissues such as tendon [17] and intestine [18] which have been analysed in tension. In both of these tissues the initial low-modulus toe region of the stress–strain curve corresponds to the progressive straightening of the planar crimped waveform of the collagen fibres. If the fibres are in a biaxial arrangement, as in the intestine, then reorientation of the fibres into the stress direction occurs simultaneously. Although it is not possible to observe the fibres directly during deformation of the disc, as was done in the tendon and intestine, it can be imagined that the initial toe region of the stress–strain curve is similarly accompanied by uncrimping of the fibres of the lamellae and reorientation into the transverse direction. Presumably, once the stress has relaxed and the lamellae have been restored at least partially to their original orientation, some recrimping of the fibres occurs. This would explain why only partial uncrimping and reorientation are observed when the relaxed disc is fixed and sectioned for histological examination.

It is also imagined that when the fibres are fully uncrimped, further bulging of the lamellae requires the fibres to extend; this produces the linear region of the stress–strain curve. The strong dependence of the apparent modulus on loading rate is attributed primarily to water transport out of the disc as it is being compressed. At slower loading rates this occurs sufficiently quickly that the volume loss is significant on the timescale of the experiment; less bulging is then required to accommodate the compressive displacement of the vertebral bodies, and the local tensile strain experienced by the fibres is reduced. However, the well-known viscoelastic nature of the collagen fibres may also contribute to the rate-dependence.

4. Conclusions

This study of the relationship between the measured mechanical properties of the intervertebral disc and the hierachical structure has led to the following conclusions regarding the response of the disc system to compressive deformation.

1. It is proposed that time-dependent features of the mechanical response, specifically the effect of the loading rate on the stress–strain relationship and the stress-relaxation behaviour, are due to a decrease in volume of the disc caused by stress-driven transport of water out of the disc through the cartilage end-plates into the vertebral bone.

2. Lateral bulging of the nucleus forces the disc to bulge outwards when compressed. Bulging of the peripheral lamellae is minimized by the curvature of the vertebral interface, which causes the disc height to be greatest at the periphery, and by the gradient of water content, which causes water to be lost preferentially from the inner lamellae and nucleus when the disc is compressed.

3. When the disc bulges, the fibres of the lamellae are loaded in tension and their mode of deformation is similar to that of other connective tissues, such as tendon and intestine, that have been analysed in tension. The initial low-modulus region of the stress–strain curve is associated with straightening of the crimped waveform and reorientation of fibres into the

transverse direction, whereas the linear modulus region is identified with extension of the straightened fibres.

Acknowledgement

This research was generously supported by the Army Research Office, grant number DAAL03-88K-0097.

References

1. J. J. CASSIDY, A. HILTNER and E. BAER, *Connect. Tissue Res.* **23** (1989) 75.
2. J. DIAMANT, *et al.*, *Proc. R. Soc.* **B180** (1972) 293.
3. J. ORBERG, E. BAER and A. HILTNER, *Connect. Tissue Res.* **11** (1983) 285.
4. W. J. VIRGIN, *J. Bone Joint Surg.* **B33** (1951) 607.
5. T. BROWN, R. J. HANSEN and A. J. YORRA, *ibid.* **A39** (1957) 1135.
6. K. L. MARKOLF and J. M. MORRIS, *ibid.* **A56** (1974) 675.
7. L. E. KAZARIAN, *Orthop. Clin. N. Amer.* **6** (1975) 3.
8. W. KOELLER, W. MEIER and F. HARTMANN, *Spine* **9** (1984) 725.
9. A. L. NACHEMSON, A. B. SCHULTZ and M. H. BERKSON, *ibid.* **4** (1979) 1.
10. P. BRINCKMANN and M. HORST, *ibid.* **10** (1985) 138.
11. M. REUBER, *et al.*, *J. Biomech. Eng.* **104** (1982) 187.
12. J. A. KLEIN and D. W. L. HUKINS, *Biochim. Biophys. Acta* **717** (1982) 61.
13. D. S. HICKEY and D. W. L. HUKINS, *Spine* **5** (1980) 106.
14. J. P. G. URBAN and J. F. McMULLIN, *ibid.* **13** (1988) 180.
15. W. KOELLER, F. FUNKE and F. HARTMANN *Biorheology* **21** (1984) 675.
16. J. J. CASSIDY, *et al.*, *J. Mater Sci.: Mater. Med.* **1** (1990) 81.
17. J. KASTELIC and E. BAER, in "The Mechanical Properties of Biological Materials", edited by J. F. V. Vincent and J. D. Currey (Society of Experimental Biology, London, 1980) p. 397.
18. K. FACKLER, L KLEIN and A. HILTNER, *J. Microsc.* **124** (1981) 305.

Received 8 December 1989
and accepted 10 January 1990